A μ^+SR study of the rare earth antiferromagnet PrO_2

2003 J. Phys.: Condens. Matter 15 8407

(http://iopscience.iop.org/0953-8984/15/49/017)

INSTITUTE OF PHYSICS PUBLISHING JOURNAL OF PHYSICS: CONDENSED MATTER

J. Phys.: Condens. Matter **15** (2003) 8407–8415 PII: S0953-8984(03)70866-2

A μ^+SR study of the rare earth antiferromagnet PrO_2

T Lancaster[1], S J Blundell[1], F L Pratt[2], C H Gardiner[3], W Hayes[1] and A T Boothroyd[1]

[1] Clarendon Laboratory, Parks Road, Oxford OX1 3PU, UK
[2] ISIS Muon Facility, Rutherford Appleton Laboratory, Chilton, Didcot OX11 0QX, UK
[3] National Physical Laboratory, Queens Road, Teddington, Middlesex TW11 0LW, UK

E-mail: t.lancaster1@physics.ox.ac.uk

Received 22 October 2003
Published 25 November 2003
Online at stacks.iop.org/JPhysCM/15/8407

Abstract

We present zero-field muon spin relaxation (μ^+SR) measurements on the rare earth antiferromagnet PrO_2. Oscillations in the time dependence of the muon polarization, characteristic of a quasistatic magnetic field at two distinct muon sites, are observed below T_N, along with relaxation dominated by the magnitude of the local field. Candidate muon sites in the material are suggested on the strength of dipole field calculations. Relaxation above T_N allows a prediction of the quasielastic neutron scattering linewidth, which is discussed in terms of a simple model of magnetoelastic relaxation involving a crystal field state at an energy Δ above the ground level. The obtained value of Δ may be taken as an approximate estimate of the splitting of the Γ_8 ground state of Pr^{4+} in the distorted fluorite structure.

1. Introduction

PrO_2 is an insulator with the fluorite structure, and exhibits type-I antiferromagnetic (AFM) ordering below $T_N = 14$ K with an anomalously low ordered moment of $\sim 0.6\ \mu_B$ [1]. The electronic ground state of PrO_2 has been discussed for many years [2, 3], but recent neutron spectroscopic measurements of the magnetic excitations in PrO_2 have added a new twist to the story [4]. These measurements reveal sharp peaks characteristic of transitions between levels of the $4f^1$ configuration of Pr^{4+} split by the cubic crystal field, together with broad bands of scattering centred near 30 and 160 meV. A simple model based on a vibronic Hamiltonian accounts for the main features of the data. It showed that $90 \pm 10\%$ of the Pr^{4+} ions have a localized $4f^1$ configuration, and that the broad bands of scattering result from a mixing of electronic and lattice degrees of freedom driven by coupling between $4f^1$ electronic states and local dynamic distortions. This effect has been explained by a dynamic Jahn–Teller effect [4].

Another recent development is the discovery of a distortion of the oxygen sublattice on cooling to $T_D = 120$ K, believed to be due to the cooperative Jahn–Teller effect [5]. Since

the ground state comprises mixed electronic and vibrational degrees of freedom, structures involving coupled magnetic ordering and lattice distortions may occur at low temperatures.

A muon spin relaxation (μ^+SR) study on PrO_2, where magnetoelastic coupling is important [4], provides an opportunity to examine the effect of this coupling on local static and dynamic magnetic properties. In particular, the muon can be used to study the magnetic fluctuations of the Pr^{4+} moments, which are in turn strongly coupled to the lattice. The muon is sensitive to low frequency fluctuations and therefore may give information on very low-lying crystal field levels.

2. Experimental details

μ^+SR experiments were carried out on the EMU instrument at the ISIS facility, Rutherford Appleton Laboratory, Didcot, UK and on the GPS instrument at the Paul Scherrer Institute (PSI), Villigen, Switzerland.

In a μ^+SR experiment [6] spin-polarized positive muons are stopped in a target sample, where the muon usually occupies an interstitial position in the crystal. The observed property in the experiment is the time evolution of the muon spin polarization, the behaviour of which depends on the local magnetic field at the muon site. Each muon decays, with a lifetime of 2.2 μs, into two neutrinos and a positron, the latter particle being emitted preferentially along the instantaneous direction of the muon spin. Recording the time dependence of the positron emission directions therefore allows the determination of the spin polarization of the ensemble of muons.

In our experiments positrons are detected by detectors placed forward (F) and backward (B) of the initial muon polarization direction. Histograms $N_F(t)$ and $N_B(t)$ record the number of positrons detected in the two detectors as a function of time following the muon implantation. The quantity of interest is the decay positron asymmetry function, defined as

$$A(t) = \frac{N_F(t) - \alpha N_B(t)}{N_F(t) + \alpha N_B(t)}\,, \tag{1}$$

where α is an experimental calibration constant. $A(t)$ is proportional to the spin polarization of the muon ensemble.

Powder samples (prepared as described in [4]) of typical mass 0.3 g were packed in silver foil and mounted on a silver sample holder. Silver is used because the low nuclear moment of silver does not cause a significant relaxation of the muon spin.

3. Results and discussion

A zero-field (ZF) μ^+SR asymmetry spectrum for times $0 \leqslant t \leqslant 0.3$ μs (measured at PSI) is shown in figure 1. Spectra measured at $T < T_N$ show oscillations due to a quasistatic internal magnetic field at the muon site, which causes a coherent precession of the spins of those muons with a component of their polarization perpendicular to this local field. Two separate frequencies were observed in the spectra, corresponding to two distinct muon sites in the crystal.

The spectra may be fitted to an expression of the form

$$A(t) = A_\parallel \exp(-\lambda_\parallel t) + A_1 \exp(-\sigma_1^2 t^2)\cos(2\pi\nu_1 t + \phi_1) + A_2 \exp(-\sigma_2^2 t^2)\cos(2\pi\nu_2 t + \phi_2) \tag{2}$$

with $2\pi\nu_i = \gamma_\mu B_i$, where γ_μ is the muon gyromagnetic ratio ($\equiv 2\pi \times 135$ MHz T^{-1}) and B_i is the local field at the ith muon site. The oscillatory terms describe the precession of the

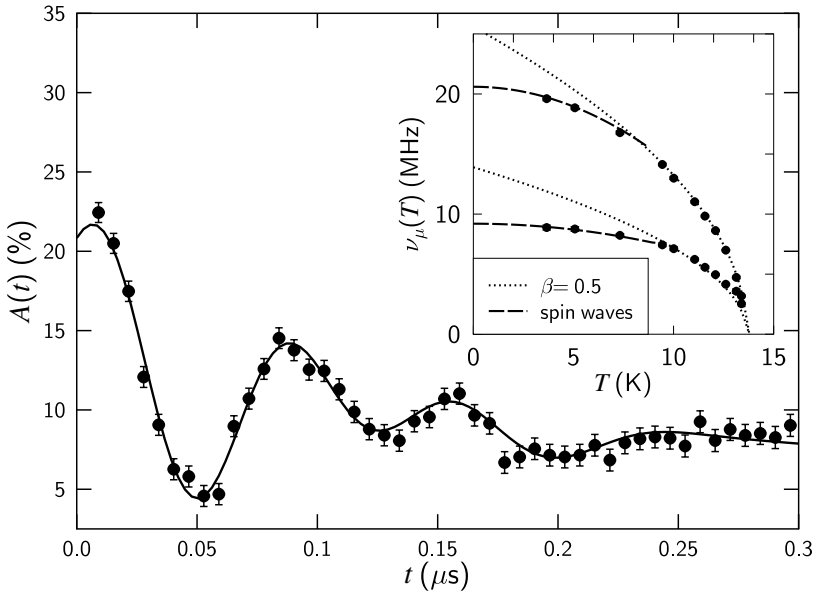

Figure 1. ZF μ^+SR spectrum measured at 5 K showing oscillations due to magnetic order. Inset: the variation of the precession frequencies ν_i with temperature. Fits are shown to mean field theory and AFM spin wave theory.

muon in the local field, while the relaxation of the signal is due to any distribution in the fields experienced by different muons in the ensemble. We note that two oscillatory frequencies were also detected in UO_2 [7], which also has a slightly distorted fluorite structure at low temperatures [8]. Two oscillatory frequencies imply two magnetically inequivalent muon sites (see below). The Gaussian form of the relaxation is typical of a quasistatic distribution of local moments. The amplitudes A_1 and A_2 were found to be in a ratio of roughly 2:1.

The temperature evolution of the precession frequencies is shown in the inset of figure 1. Close to the critical region, the temperature dependence was well described by the functional form

$$\nu_\mu(T) \propto (1 - T/T_N)^\beta, \tag{3}$$

where β was found to be 0.5(1) with $T_N = 13.7(2)$ K. While $T_N = 13.7(2)$ K agrees (within experimental uncertainty) with the value extracted from the most recent neutron diffraction study [5], there is a discrepancy between the value of $\beta = 0.28$ extracted from neutron diffraction data and the value presented here. This may be attributable to the difficulty in fitting muon spectra near a critical point or to the limited temperature range over which β was extracted. In view of this, β is best viewed as a phenomenological parameter characterizing the data rather than as a precise critical parameter. At low temperatures we fit the frequency $\nu_\mu(T)$ to AFM spin wave theory, which predicts

$$\nu_\mu(T) = \nu_i(0)(1 - \xi(T/T_N)^2), \tag{4}$$

with $\xi = 0.5(2)$ (corresponding to an exchange constant of order $J/k_B \sim 5$ K), $\nu_1(0) = 20.3(1)$ MHz (equivalent to a local field at the muon site of 150(1) mT) and $\nu_2(0) = 10(1)$ MHz (equivalent to 73(7) mT).

The relaxation rates σ_i ($= \gamma_\mu \Delta B/\sqrt{2}$) appear to be the sum of two terms. The first has a similar temperature dependence to the precession frequency (which suggests that this term is

dominated by the magnitude of the local field distribution), while the second is a temperature independent offset. If the static field distribution responsible for the damping scales only with frequency (i.e. $\Delta B = C\nu_i(T)$, where C is independent of both ν_i and T), then we would expect

$$\sigma_i(T) = \frac{\gamma_\mu C}{\sqrt{2}}\nu_i(T) + \sigma_i^{\mathrm{bg}}, \tag{5}$$

where σ_i^{bg} is the constant offset term. Values of σ_i^{bg} were determined from the data to be $\sigma_1^{\mathrm{bg}} \approx 2.5$ MHz and $\sigma_2^{\mathrm{bg}} \approx 1.5$ MHz. The temperature dependence of σ_1 and σ_2 is illustrated in figure 2(a), and the scaled quantity $(\sigma_i(t) - \sigma_i^{\mathrm{bg}})/\nu_i(0)$ is plotted as a function of temperature in figure 2(b). While the precise origin of σ_i^{bg} is not clear at present, at least a substantial fraction of the temperature independent relaxation can be attributed to the Pr nuclear dipoles.

The longitudinal relaxation, parameterized by a single relaxation rate, $\lambda_\parallel = 2\gamma_\mu^2(\Delta B)^2\tau$, where $1/\tau$ is the field fluctuation rate, was also found to be dominated by the magnitude of the field distribution (see figure 2(c)), suggesting that τ is only weakly temperature dependent in the ordered state.

In our fits A_1, A_2 and $A_\parallel$ were held constant. We found the best fits for $A_\parallel/(A_1{+}A_2) = 1.1$. This is larger than the expected vale of 0.5, but this may be due to a greater complexity in the relaxation function than considered in equation (2), the presence of some additional relaxing fraction in the sample, or it may be an artefact resulting from possible distortions in the data at very early times.

Alternative interpretations of the data below T_{N} were considered, including the possibility of incommensurate magnetic order, although these resulted in significantly worse fits to the measured spectra.

Our measurement of $\nu_i(0)$ allows us to attempt to determine the muon sites in PrO_2. The magnetic field at a muon site $\mathbf{B}_\mu(\mathbf{r}_\mu)$ is given by the sum of dipolar contributions. Assuming that the local field is due entirely to the dipole field of Pr ions,

$$\mathbf{B}_\mu(\mathbf{r}_\mu) = \sum_i \frac{3(\boldsymbol{\mu}_i \cdot \hat{\mathbf{n}}_i)\hat{\mathbf{n}}_i - \boldsymbol{\mu}_i}{|\mathbf{r}_\mu - \mathbf{r}_i|^3}, \tag{6}$$

where $\mathbf{r}_\mu$ is the position of the muon, $\boldsymbol{\mu}_i$ is the ordered magnetic moment of the ith Pr ion and $\hat{\mathbf{n}}_i$ $(=(\mathbf{r}_\mu - \mathbf{r}_i)/|\mathbf{r}_\mu - \mathbf{r}_i|)$ is the unit vector from the muon to the Pr ion at site $\mathbf{r}_i$. The positive muon's position is usually in the vicinity of the electronegative O^{2-} ions [9].

The exact magnetic structure of PrO_2 is unknown and the available neutron data are consistent with either 1-k, 2-k or 3-k transverse type-I magnetic structures [10], together with a second component with twice the period along one axis [5]. Although we might assume the 3-k structure of UO_2 [11], the dipole field calculation yields consistent sites for 2-k and 1-k structures as well. The best candidate sites, for all three structures, lie near oxygen positions in the a–b plane, removed from them along the c-axis by ± 0.9 Å (an example is shown in figure 3). At these positions, both observed frequencies are found in equal proportions (note that one frequency will be found at +0.9 Å, the other at -0.9 Å). The symmetry of the crystal requires that the general muon position, consistent with that suggested above, be at the centre of a face of the cube (of edge length $\approx$1.8 Å) centred on an oxygen ion. However, for the 2-k and 1-k magnetic structures, these symmetry-related sites are magnetically inequivalent [11] and produce not only the observed frequencies, but others as well. This is not the case for the 3-k structure, so that this interpretation therefore favours the 3-k structure. Whereas this analysis should result in spectra with equal amplitudes A_1 and A_2 (which is not observed; see above), the situation must be somewhat more complicated than considered in this interpretation.

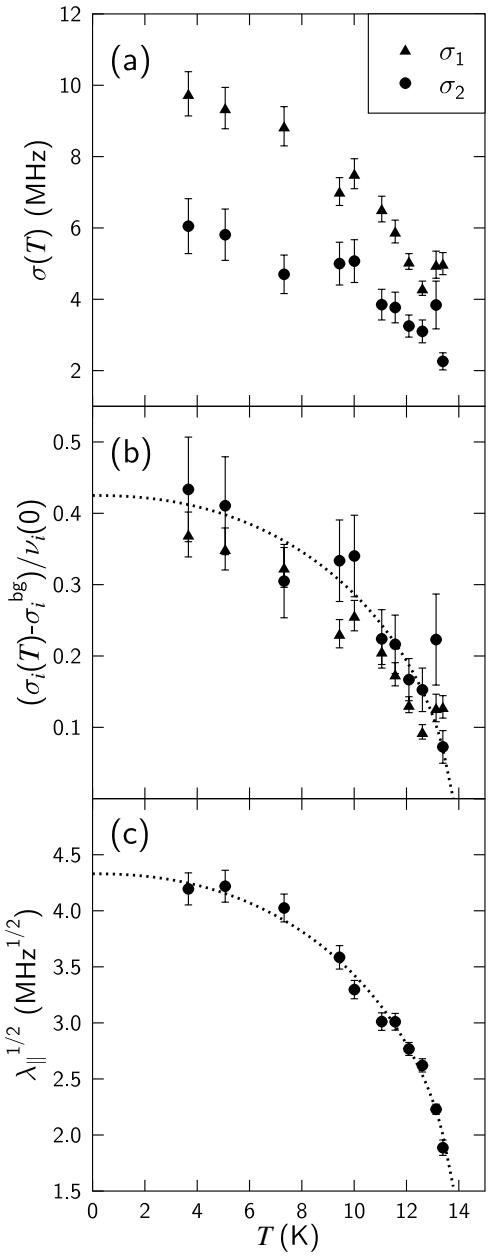

Figure 2. (a) Relaxation rates σ_i as a function of temperature. (b) Scaled relaxation rates $(\sigma_i(t) - \sigma_i^{bg})/\nu_i(0)$ as a function of temperature, showing that the relaxation rates are dominated by the contribution due to the magnitude of the magnetic field at the ith muon site. The dotted curve shows the behaviour expected from equation (5). (c) The temperature dependence of $\sqrt{\lambda_\parallel}$, again showing behaviour dominated by the magnitude of the magnetic field distribution.

Asymmetry spectra for times $0 \leqslant t \leqslant 10$ μs (measured at ISIS) allow the relaxation above T_N to be studied. Data were recorded from T_N up to 250 K and were found to fit best to a function of the form

$$A(t) = A\exp(-\Lambda t), \tag{7}$$

which is characteristic of dynamic relaxation involving a single fluctuation rate (we do not see two separate relaxation rates corresponding to the two muon sites in the material). Further evidence that the observed behaviour is dynamic in origin is provided by the observation that

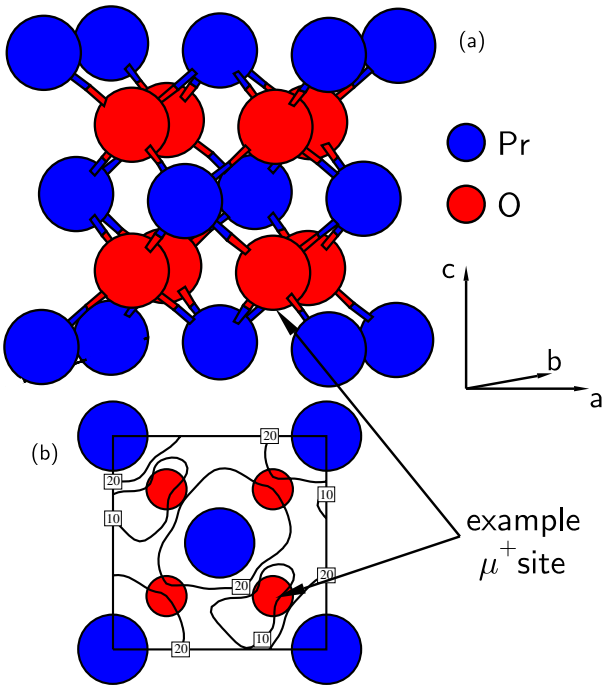

Figure 3. (a) The room temperature crystal structure of PrO_2 showing the proposed muon sites. (b) A dipole field contour map at $z = 0.09c$ for the 3-k magnetic structure. Contours of $\nu_0 = 20$ MHz and $\nu_0 = 10$ MHz are labelled. An example μ^+ site is shown with $\nu(0) = 10$ MHz. Further sites can be obtained using the four-fold rotation axis about the central Pr atom and these also have precession frequencies close to either 10 or 20 MHz. Analogous sites are obtained in the planes $z = 0.41c$, $0.59c$ and $0.91c$. The 3-k magnetic structure breaks the symmetry between muon sites above and below the planes of oxygen atoms.

(This figure is in colour only in the electronic version)

applied magnetic fields as high as 200 mT do not decouple the relaxation (decoupling implies $\lim_{t\to\infty} A(t) = A(0)$, which is not observed).

Figure 4(a) shows the behaviour of Λ with T. The relaxation rate Λ diverges as we approach T_N from above, demonstrating that the magnetic fluctuations which give rise to the relaxation of the muon spin polarization slow down as the transition is approached. The relaxation rate Λ may be written in terms of the response function $S(\mathbf{q}, \omega)$ [12, 13] as

$$\Lambda \propto \sum_{\mathbf{q}} G^2(\mathbf{q}) S(\mathbf{q}, 0), \tag{8}$$

where $G(\mathbf{q})$ is the $\mathbf{q}$-dependent coupling [14] which depends on the muon site and encodes the local geometry around this site, but is frequency independent (and can be taken to be independent of temperature). Equation (8) is a sum over all wavevectors $\mathbf{q}$ because the muon is a local probe. Using the fluctuation–dissipation theorem, it is possible to show that [12–15]

$$\Lambda \propto k_B T \sum_{q} \frac{G^2(\mathbf{q})\chi(\mathbf{q}, 0)}{\Gamma(\mathbf{q})}, \tag{9}$$

where $\chi(\mathbf{q}, 0)$ is the static susceptibility and $\Gamma(\mathbf{q})$ is the quasielastic linewidth obtainable from a neutron scattering experiment.

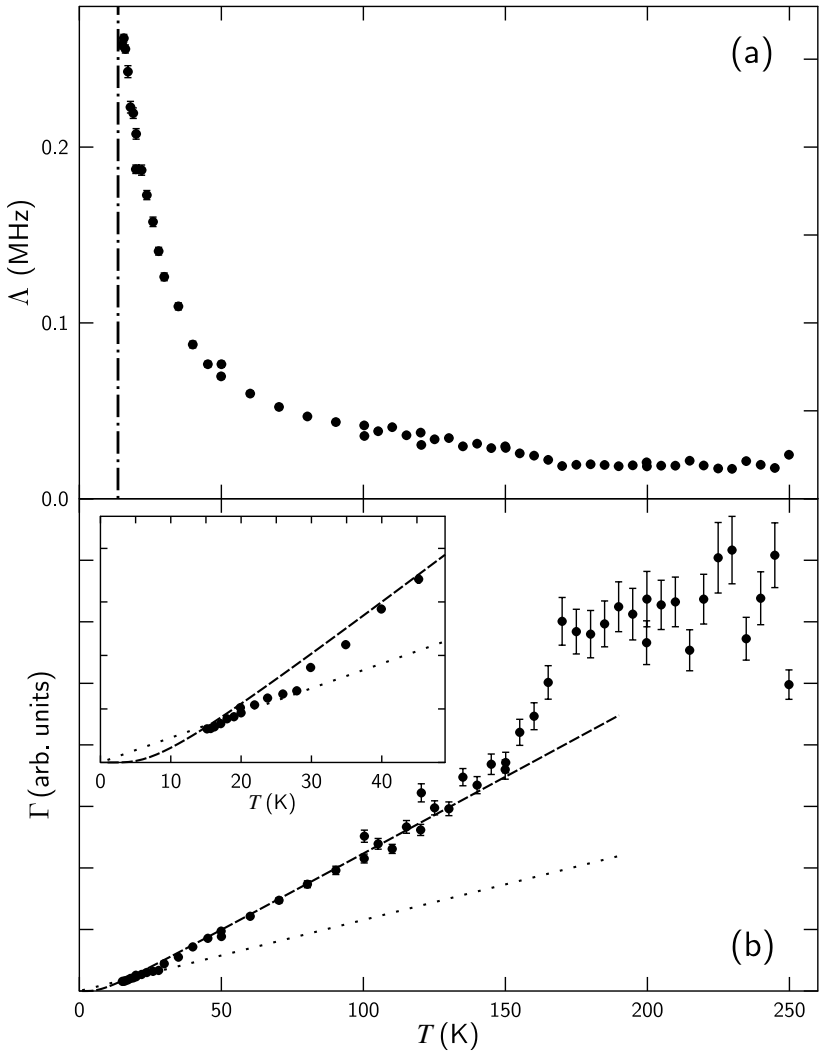

Figure 4. (a) The variation of the relaxation rate Λ above T_N, diverging as $T \to T_N$ from above. (b) The estimated neutron scattering quasielastic linewidth, calculated from the muon relaxation rate and bulk magnetic susceptibility (from [5]). Fits are shown to $\Gamma = aT$ (dotted line) and equation (11) (dashed line). Inset: detail from (b) for $0 \leqslant T \leqslant 50$ K.

If we assume a weak **q**-dependence for both $\Gamma(\mathbf{q})$ and $G(\mathbf{q})$, then the experimentally measured bulk magnetic susceptibility $\chi_0 = \sum_{\mathbf{q}} \chi(\mathbf{q}, 0)$ [5] allows us to estimate the temperature variation of the quasielastic linewidth Γ, according to

$$\Gamma = \frac{\alpha \chi_0 T}{\Lambda}, \tag{10}$$

where α is a constant. This is shown in figure 4(b), where we see that Γ varies approximately linearly with temperature over the region 14–160 K, becoming less well defined at higher temperatures (where the assumption of weak **q**-dependence is expected to break down and additional contributions to Λ become significant).

The relaxation of the Pr^{4+} moments is dominated by modulation of the orbital motion of the valence electrons by thermally activated relative motion between Pr^{4+} and O^{2-} ions. This magnetoelastic relaxation mechanism is particularly effective because of the large spin–orbit interaction in Pr^{4+}. A similar type of relaxation was recently proposed to explain the neutron scattering linewidth of lanthanide ions doped into $YBa_2Cu_3O_{6+x}$ [16] and described using a three-state model [17] which is not unlike Orbach's two phonon relaxation [18]. This treatment demonstrated that

$$\Gamma \propto (\exp(\Delta/k_B T) - 1)^{-1}, \tag{11}$$

where Δ is the energy of an intermediate crystal field state, which in this case may possibly be related to the expected splitting of the four-fold degenerate Γ_8 ground state into two doublets by the distortion at 120 K. This model can be improved by including more intermediate levels in the calculation [19]. Our estimate for Γ is only available above T_N, but fitting the temperature dependence of Γ from T_N up to 130 K to equation (11) produces a reasonably good fit and yields $\Delta = 2.0$ meV, though the fit overestimates Γ slightly in the region near 30 K. In contrast, attempts to fit the straight line form $\Gamma = aT$ over the same range result in a very poor fit, except below 30 K, as shown in figure 4(b). It would be desirable to include more relaxation channels into this model in order to provide a better assessment of the importance of magnetoelastic relaxation, but this is difficult without knowing more about the phonon density of states and the magnetoelastic coupling strengths for individual phonon modes [19].

We note, finally, that no feature is observed in the muon spin relaxation at the lattice distortion temperature $T_D = 120$ K. We conclude that the distortion in the oxygen sublattice appears to have little effect on the spin fluctuations which cause the measured relaxation of the muon spin above T_N.

4. Conclusions

The temperature dependence of the local field in the magnetically ordered phase of PrO_2 ($T_N = 13.7$ K) has been studied along with the fluctuations in both ordered and disordered phases. Dipole field calculations suggest muon sites near oxygen positions in the *a*–*b* plane, displaced along the *c*-direction from the oxygen sites by $\approx \pm 0.9$ Å. The relaxation rate in the disordered phase above T_N, when taken with susceptibility data, allows a prediction of the temperature dependence of the neutron scattering quasielastic linewidth Γ. This fits to a simple model of magnetoelastic relaxation, with an intermediate crystal field state at $\Delta = 2.0$ meV. Our value of Δ may be taken as an approximate estimate of the splitting of the four-fold degenerate Γ_8 ground state of Pr^{4+} in the cubic crystal into two doublets by the distortion at 120 K.

Acknowledgments

We are grateful to Steve Cottrell at ISIS and Alex Amato at PSI for technical assistance. This work was funded by the EPSRC.

References

[1] Kern S, Loong C-K, Faber J Jr and Lander G H 1984 *Solid State Commun.* **49** 295
[2] Kotani A, Jo T and Parlebas J C 1988 *Adv. Phys.* **37** 37
[3] Wuilloud E, Delly B, Schneider W-D and Baer Y 1984 *Phys. Rev. Lett.* **53** 202
Marabelli F and Wachter P 1987 *Phys. Rev.* B **36** 1238

[4] Boothroyd A T, Gardiner C H, Lister S J S, Santini P, Rainford B D, Noailles L D, Currie D B, Eccleston R S and Bewley R I 2001 *Phys. Rev. Lett.* **86** 2082
[5] Gardiner C H, Boothroyd A T, Pattison P, McKelvy M J, McIntyre G J and Lister S J S 2003 *Phys. Rev.* B, submitted
[6] Blundell S J 1999 *Contemp. Phys.* **40** 175
[7] Kopmann W, Litterst F J, Klauß H-H, Hillberg M, Wagener W, Kalvius G M, Schreier E, Burghart F J, Rebizant J and Lander G H 1998 *J. Alloys Compounds* **271** 463
[8] Faber J Jr and Lander G H 1976 *Phys. Rev.* B **14** 1151
[9] Li Q and Brewer J H 1990 *Hyperfine Interact.* **63** 169
[10] Gardiner C H, Boothroyd A T, Lister S J S, McKelvy M J, Hull S and Larsen B H 2002 *Appl. Phys.* A **74** S1773
[11] Giannozzi P and Erdös P 1987 *J. Magn. Magn. Mater.* **67** 75
[12] Blundell S J and Cox S F J 2001 *J. Phys.: Condens. Matter* **13** 2163
[13] Lovesey S W 1984 *Theory of Neutron Scattering from Condensed Matter* (Oxford: Oxford University Press)
[14] Dalmas de Rotier P and Yaouanc A 1997 *J. Phys.: Condens. Matter* **9** 9113
[15] Chaikin P M and Lubensky T C 1995 *Principles of Condensed Matter Physics* (Cambridge: Cambridge University Press)
[16] Staub U, Gutmann M, Fauth F and Kagunya W 1999 *J. Phys.: Condens. Matter* **11** L59
[17] Lovesey S W and Staub U 2000 *Phys. Rev.* B **61** 9130
[18] Orbach R 1961 *Proc. R. Soc.* A **264** 458
[19] Boothroyd A T 2001 *Phys. Rev.* B **64** 066501